Available online at www.sciencedirect.com

SCIENCE DIRECT®

Vision Research 44 (2004) 3253–3268

Vision Research

www.elsevier.com/locate/visres

# In vivo studies of signaling in rod pathways of the mouse using the electroretinogram

J.G. Robson, H. Maeda, S.M. Saszik, L.J. Frishman *

*College of Optometry, University of Houston, Houston, TX 77204-2020, USA*

Received 24 June 2004; received in revised form 8 September 2004

**Abstract**

*Purpose:* (a) To examine the possibility that there is a threshold in the synaptic mechanism linking rods to rod bipolar cells that can reduce the transmission of continuous noise from the rods without blocking the transmission of any significant proportion of single-photon responses. (b) To estimate the level of this threshold and the amplitude of the continuous noise which it can serve to reduce. (c) To identify the location of the threshold mechanism in the rod to rod bipolar cell pathway.

*Methods:* Corneal electroretinogram recordings were made from dark-adapted mice anesthetized with ketamine/xylazine after inner-retinal components had been suppressed to isolate PII, the response of depolarizing bipolar cells. Suppression was achieved by intravitreal injections of GABA, TTX, or in Cx36 KO animals by crushing the optic nerve and waiting for ganglion cells to degenerate.

*Results:* All energy-scaled records of isolated PII obtained with ganzfeld stimuli that gave rise to much less than one photoisomerization (R*) per rod (0.01–0.2 R*/rod), had an essentially identical waveform. Stronger stimuli caused a reduction in the peak amplitude of energy-scaled records (saturation) and stimuli strong enough to produce multiple isomerizations in individual rods resulted in a shortening of the response latency and an increase of the energy-scaled amplitude at early times (supralinearity). The shape of the rising edge of isolated PII changed with flash energy in a way that was consistent with the existence of a synaptic threshold whose level was less than one tenth of the amplitude of single-photon signals and a continuous noise whose rms amplitude was even less than this. However, when measured at the time of the peak, the amplitude of PII increased linearly in proportion to stimulus energy from the very lowest levels up to the point where there was, on average, 0.2 R*/rod.

*Conclusions:* There is a threshold nonlinearity operating at the output of the rod to rod bipolar cell synapse that can usefully reduce the transmission of continuous rod noise without significantly affecting the transmission of single-photon signals. This nonlinearity does not affect the overall linear function of the rod pathway at levels at which it is effectively operating in a photon-counting mode.



*Keywords:* Rod bipolar cell; Threshold nonlinearity; Electroretinography; Rod pathway

## 1. Introduction

The ability of the visual system to achieve the highest possible visual sensitivity requires that the signals produced by the absorption of single photons in individual rods should be reliably signaled to the brain. If such reliable signaling can be realized then the only peripheral limit to visual sensitivity will be the rate at which molecules of rhodopsin spontaneously undergo the isomerization that is normally associated with activation by single photons.

To achieve this performance it is necessary that the transient electrical response of each rod to activation of

* Corresponding author. Address: College of Optometry, University of Houston, 505 J Davis Armistead, Houston, TX 77204-2020, USA. Tel.: +1 713 743 1972; fax: +1 713 743 2595.

*E-mail address:* lfrishman@uh.edu (L.J. Frishman).

0042-6989/$ - see front matter © 2004 Elsevier Ltd. All rights reserved.
doi:10.1016/j.visres.2004.09.002

a single molecule of rhodopsin should be large enough to be reliably discriminated from the spontaneous electrical noise that results from the operation of the biochemical cascade that serves to amplify the effect of the initial molecular event. Although this is a necessary requirement, and one that is certainly achieved in fully dark-adapted mammalian rods, it is not, of itself, sufficient to ensure optimal visual sensitivity because the rod signals are not directly relayed to the brain. Rather, signals from many hundreds, or thousands, of rods are collected together in three successive stages in the retina before being signalled to the brain by the ganglion cell discharge. If this high degree of signal convergence is not to result in single-photon signals from activated rods becoming submerged in the noise coming from the much larger number of nonactivated rods or from the operation of the intermediary synapses, then the main rod pathway cannot simply add the rod signals together. Instead, it must operate in some other way to reduce the transmission of noise relative to the transmission of photon signals.

The first stage of convergence of rod signals in the mammalian retina is provided by the rod bipolar cells which each receive inputs from 20–25 rods (e.g. Sterling, Freed, & Smith, 1988 for cat; Wässle, Grünert, Chun, & Boycott, 1995 for monkey; Tsukamoto, Morigiwa, Ueda, & Sterling, 2001 for mouse). If these inputs were in effect simply added then the signal-to-noise ratio at the output of the bipolar cell would be reduced relative to that of the rods themselves by a factor of 5 or so (the square root of the number of converging inputs), a reduction that would certainly militate against the reliable signaling of the absorption of a single photon event within the input ensemble. As an alternative it has been suggested that there is a threshold nonlinearity at the synapse that connects each rod to a rod bipolar cell so that little or none of the lower amplitude "continuous noise" in each rod output is transmitted to the bipolar cell (Baylor, Nunn, & Schnapf, 1984; van Rossum & Smith, 1998). In this way the initial stage of rod signal convergence could be achieved without significant reduction of signal-to-noise ratio.

While the operation of such a threshold has been observed directly in recordings from rod bipolar cells in mouse retinal slices (Field & Rieke, 2002) and the threshold level estimated to be approximately the same as the peak amplitude of a single-photon response, previous studies of the rod bipolar cell component of the cat electroretinogram (ERG) did not indicate the existence of such a high threshold in cat retina (Robson & Frishman, 1995). We have now examined the ERG of mice for evidence of such a threshold and find clear indications that such a threshold exists, but that it is of a much lower level than suggested by Field and Rieke's (2002) observations in mouse retinal slice preparations. We have also estimated the amplitude of the continuous noise relative to the single-photon response and found this to be substantially lower than reported by Field and Rieke (2002) in mouse rods in vitro.

## 2. Methods

Preparation, recording and injection methods were described in a previous publication, Saszik, Frishman, and Robson (2002) and will be described only briefly here. Recordings were made from seven c57BL6 mice and two Connexin36 knockout mice (Cx36 KO; Deans, Volgyi, Goodenough, Bloomfield, & Paul, 2002). Adult mice initially were anesthetized with an intraperitoneal injection of ketamine (60 mg/kg) and xylazine (6 mg/kg), and anesthesia was maintained with ketamine (56 mg/kg) and xylazine (5.6 mg/kg) given every 45–60 min via a subcutaneous needle fixed in the flank. The nose was clamped lightly with the two front teeth held in a metal bite bar that also served as the electrical ground. Pupils were fully dilated to 3 mm in diameter with topical atropine (0.5%) and phenylephrine (2.5%). Rectal temperature was maintained at 37–38 °C. Recording sessions lasted 4–8 h. Nearly all of the mice were allowed to recover from anesthesia after each session. All experimental and animal care procedures adhered to the ARVO Statement for the Use of Animals in Ophthalmic and Vision Research and were approved by the Institutional Animal Care Committee of the University of Houston.

ERG recordings were made differentially between DTL fiber electrodes (Dawson, Trick, & Litzkow, 1979) placed across the center of the cornea of each eye. The electrodes were moistened with methylcellulose sodium (Celluvisc, Allergan Inc., USA) to keep the corneas hydrated and to ensure good electrical contact. The cornea of the tested eye was covered with a clear contact lens, the nontested eye with a black contact lens and a black aluminum foil cap that covered both the eye and the skull. Animals were dark-adapted overnight and prepared for recording under red illumination (LED, $\lambda > 640$ nm).

The ganzfeld ERG stimulus consisted of brief (0.8 μs to 4.1 ms) full-field flashes (LEDs, $\lambda_{max} = 462$ nm) from stimuli too weak to produce measurable responses (−6.1 log scotopic Troland seconds (sc Td s)) to strong stimuli (1.8 log sc Td s) that elicited a-waves. The interval between flashes was adjusted so that the ERG had returned to baseline before another stimulus was presented. The ganzfeld stimulus was produced by rear illumination of a concave white diffuser (35 mm diameter) positioned close to the eye. Time zero was taken as half-way through the flash. Responses were averaged over many trials when stimuli were weak and responses were small and over fewer trials when responses were larger. Signals were amplified from 0 to 300 Hz, digitized with a resolution of 1 μV at a rate of 1 kHz and digitally filtered offline to remove 60 Hz. A scotopically corrected

photometer (International Light model IL1700), was used to measure the luminance (sc cd $m^{-2}$) and luminous energy (sc cd s $m^{-2}$). Conversions from Troland values to photoisomerizations per rod (R*/rod) assume that 1 sc Td s gives 122 R*/rod (Saszik, Frishman, & Robson, 2002).

### 2.1. Intravitreal injection

Under a dissecting microscope (10×) a small hole was punctured in the eye just behind the limbus with a 27-gauge needle, and a glass pipette (tip ~20 μm) was inserted through the hole and the following pharmacological agents were injected (~1–1.5 μl) using a Hamilton Microsyringe (Hamilton Company, Reno, NV, USA): GABA (32–46 mM) in six mice to suppress all inner retinal activity, TTX (tetrodotoxin citrate; 3 μM) to block $Na^+$-dependent spikes. Concentrations given assume that the vitreal volume of the adult mouse is 20 μl (Saszik, Frishman, & Robson, 2002); doses were based on those used in previous studies in mice (Saszik, Frishman, & Robson, 2002), and primates (Viswanathan, Frishman, Robson, Harwerth, & Smith, 1999). Only data obtained when the ERG had stabilized, which generally occurred within an hour after an injection, were included in this study.

### 2.2. Unilateral optic nerve crush

After the animal was anesthetized, pupils were dilated with topical atropine (0.5%) and phenylephrine (2.5%) and the animal's head was fixed in a holder. A small vessel clip was used to retract the loose skin around the eyes. Under a dissecting microscope (10×), using sterile instruments (Hot Bead Sterilizer, Fine Science Tools, Inc.), a small incision was made in the conjunctiva temporally and the optic nerve (ON) was exposed using blunt dissection. The ON was crushed with forceps for 3 s. After the forceps were removed, a drop of antimicrobial ointment (AK-Spore, Akorn USA) was applied to the conjunctiva. We confirmed via direct ophthalmoscopic inspection that there was no bleeding from retinal blood vessels around the ON head after this procedure. Recordings were done at least three weeks after the optic nerve crush when ganglion cells had degenerated (Li, Schlamp, & Nickells, 1999). Ganglion cell loss was confirmed in histological sections using immunocytochemical analyses (not shown).

## 3. Results

### 3.1. General form of mouse ERG

As in all species, the corneal ERG of the mouse that is evoked by a briefly flashed ganzfeld stimulus is the sum of the contributions from many different retinal cell types. For this reason the amplitude and timecourse of the response is strongly dependent upon the energy of the stimulus and the level of adaptation of the retina as these stimulus parameters have different effects on the responses of the different cells. In this study we have only recorded responses from dark-adapted mouse eyes and are primarily interested in the responses that are mediated by the activation of the rod pathways (diagrammed in Fig. 1B). Typical examples of ERGs

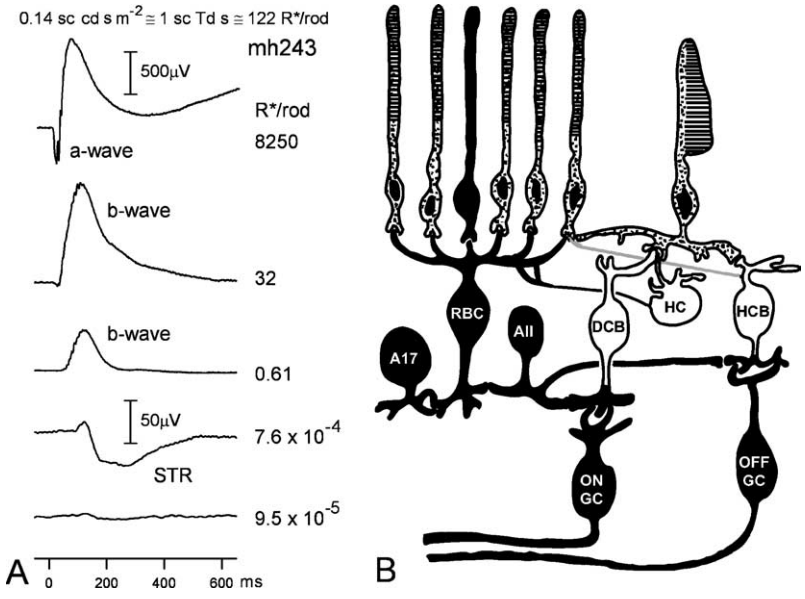


Fig. 1. Dark-adapted ERG of the mouse. (A) Typical ganzfeld flash ERG recorded from a dark-adapted mouse eye over a wide range of stimulus energies (approximately $10^{-6}$ to 70 sc Td s) producing between 1 R* per 10 000 rods and 8000 R*/rod [mh243]. (B) The principal rod pathways in the mammalian retina.

recorded with stimuli that generate such responses are shown in Fig. 1A.

The energy of the weakest ganzfeld stimulus that produces a detectable ERG in the mouse is about $10^{-6}$ scTd s and photoisomerizes only about one molecule of rhodopsin in every 10 000 rods ($10^{-4}$ R*/rod). For stimuli this weak, or just a little stronger, the recorded ERG—the scotopic threshold response (STR)—is mainly a relatively slow negative-going wave (maximal around 200 ms after the stimulus) which is preceded by a smaller brief positive wave. When the stimulus energy is increased, the negative STR soon saturates with an amplitude of 30–40 μV, while the earlier positive wave, though it also shows signs of saturating, continues to grow into the familiar b-wave of the electroretinogram. As the stimulus is increased to levels that isomerize about one rhodopsin molecule in each rod, the b-wave grows without any very obvious change in its shape although by this stimulus level its rate of growth with stimulus energy is noticeably slowing. As the stimulus energy is raised still further, an initial fast negative wave—the a-wave—appears and the amplitude of the b-wave reaches a maximum value of about 1 mV. The a-wave subsequently grows to reach a maximum amplitude of more than 0.6 mV (not illustrated) while the amplitude of the b-wave (as measured from the baseline) becomes somewhat reduced although the leading edge of the b-wave and the time-to-peak continue to become earlier and earlier.

Enough is now known about the generation of the dark-adapted ERG to be certain that the b-wave, in response to very brief flashes, is mainly provided by the activity of rod-driven depolarizing (ON) bipolar cells while the waves that are seen with the weakest stimuli are contributed by more proximal cells of the retina (Robson & Frishman, 1995, 1998; Saszik, Frishman, & Robson, 2002), and the a-wave is mainly a reflection of the earliest part of the photoreceptor response (Robson, Saszik, Ahmed, & Frishman, 2003 for review). However, because of the substantial waveform changes that accompany changes in stimulus energy, it is not immediately possible to obtain precise information about the amplitude and timing of the bipolar cell contribution to the ERG by simple measurements of responses from normal eyes. While it is possible (as will be described later) to estimate the magnitude of the photoreceptor contribution well enough to subtract it from the whole ERG in order to isolate the summed responses of the other cells, it is not yet possible to do this for the contributions from proximal retina which are less well characterized. As an alternative, we have chosen to suppress the responses of retinal cells proximal to bipolar cells pharmacologically. While various pharmacological agents (with different modes of action) are available to suppress the responses of inner retinal cells, we have found that in mice the best effect is produced by intravitreal injections of GABA (Saszik, Frishman, & Robson, 2002).

### 3.2. Effects of GABA

Fig. 2A–D (from two different animals) show respectively the effect of GABA on the mouse ERG generated in response to stimuli of low energy increasing by factors

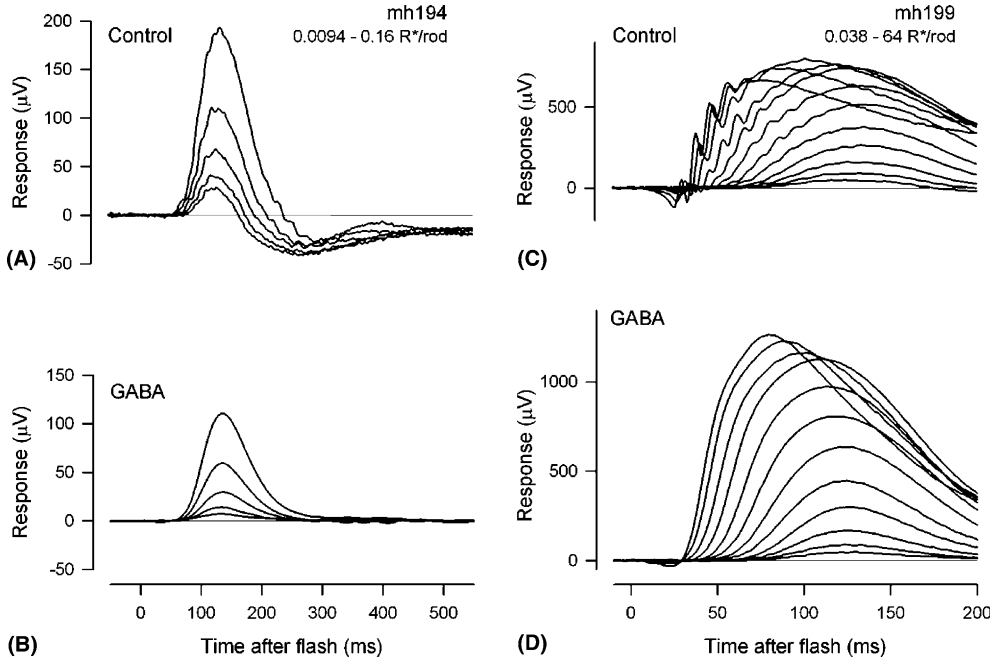


Fig. 2. ERG responses after intravitreal injection of GABA. (A and C) ERG evoked by flash stimuli of various energies prior to intravitreal injection of GABA to suppress responses of inner retinal (ganglion, amacrine and horizontal) cells. (B and D) ERG responses to the same stimuli as A and C after intravitreal injection of GABA. [(A and C), mh194 (46 mM); (B and D), mh199 (32 mM)].

of 2 from 0.0094 to 0.16 R*/rod (Fig. 2A and C) and 0.038 to 64 R*/rod (Fig. 2B and D).

Before the administration of GABA the response to weak stimuli (Fig. 2A) included a substantial negative wave following the initial positive one. Moreover, the amplitude of the positive wave did not increase in proportion to stimulus energy; in this figure the first doubling of stimulus energy produced a quite small increase in amplitude while subsequent doublings each nearly doubled the amplitude. After the intravitreal injection of GABA (Fig. 2B) the negative wave disappeared, and each doubling of stimulus energy approximately doubled the peak response amplitude but had no obvious effect on the waveform other than expected from a simple scaling. GABA also made the records smoother by removing an irregular ongoing oscillatory component normally present in the dark-adapted mouse ERG.

In response to stronger stimuli (Fig. 2C) the normal ERG shows a characteristic negative wave preceding the b-wave that is followed by stimulus-related oscillations which, for the strongest stimuli, commence at the time of the initial negative peak and are subsequently superimposed on the leading edge of the b-wave. Intravitreal GABA (Fig. 2D) greatly reduces the amplitude of the initial negative wave and completely removes the induced oscillations, as well as all ongoing oscillatory activity, making the negative peak rounder and the later records much smoother.

It is also evident in Fig. 2 that GABA reduced the amplitude of the b-wave generated by weak stimuli (presumably as a result of removing predominantly positive components generated by inner retinal cells) but increased the amplitude of the b-wave when the stimuli were stronger. The mechanism of this latter effect is unclear.

### 3.3. Comparison with in vitro bipolar cell recordings

After suppressing the responses of inner retinal cells it is to be expected that the main contributors to the ERG evoked by weak stimuli will be rod bipolar cells. In this case it is also to be expected that the waveform will be similar to the waveform that can be recorded from these cells in vitro. This expectation is confirmed by Fig. 3 which compares the normalized ERGs evoked in four animals that had received intravitreal injections of GABA with the normalized average response of 10 rod bipolar cells recorded from mouse retinal slice preparations as described by Field and Rieke (2002) and kindly made available by Dr. Rieke. The ERGs were all recorded with a stimulus energy of about 1 R*/rod while the stimulus for the in vitro recordings of cell current were made with similarly weak stimuli.

Also shown in Fig. 3 is the ERG (dashed line) recorded from a Cx36 KO mouse (Deans et al., 2002)

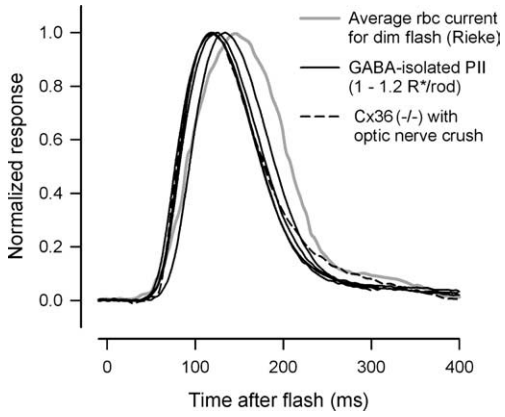


Fig. 3. Isolated PII versus rod bipolar cell responses. Isolated PII compared with the average current response to weak stimuli of rod bipolar cells in mouse retinal slices (Field & Rieke, 2002; Sampath & Rieke, 2004). ERG recordings are from four normal animals after intravitreal injection of GABA [mm216 (43 mM + TTX 3 μM), mm402 (32 mM), mh195 (32 mM) and mh199 (32 mM)] and from a Cx36 KO animal after optic nerve section [mh180].

whose optic nerve had been crushed three weeks prior to the recording. ERGs obtained in response to weak stimuli from mice with these defects lack features associated with activation of the inner retinal portion of the rod circuit (Saszik, Frishman, & Paul, 2002). The close similarity between the ERG from this mouse, the ERG from GABA-treated normal animals and the cell currents recorded in vitro, suggests that the ERG response to weak stimuli of these mice can be assumed to directly reflect the activity of rod bipolar cells alone. In fact this is not exactly correct because the ERG will include a contribution from photoreceptors, and probably also a contribution from rod-driven cone bipolar cells, though this component will presumably be absent from the ERG of the Cx36KO mice as they lack functional rod-to-cone gap junctions (Guldenagel et al., 2001; Deans et al., 2002). However, the relative amplitude of these components would be small in comparison with that of the rod bipolar cells for weak stimuli that produce no more than slight saturation of the rod bipolar cell response.

### 3.4. Linearity of the response

The indication in Fig. 2B that, after administration of GABA, the amplitude of the response to relatively weak stimuli increased linearly with stimulus energy can be confirmed by plotting amplitude as a function of stimulus energy.

Fig. 4 shows such a plot for a different animal. For low stimulus energies (from the lowest which gives a measurable response, about 0.002 R*/rod, up to about 0.2 R*/rod) the peak response amplitude is well described as increasing in proportion to stimulus energy. At higher levels (but still a very low level in absolute

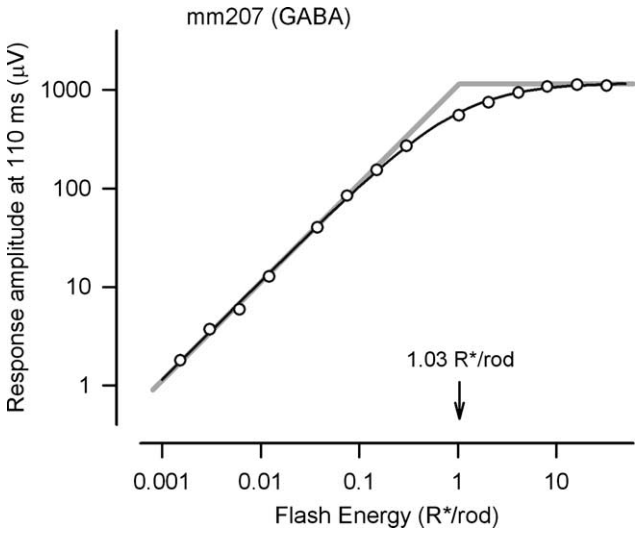


Fig. 4. Peak amplitude of the ERG of a normal animal after intravitreal injection of GABA as a function of stimulus energy. The continuous curve (hyperbolic saturation) has the form $V = V_{max}E/(E_0 + E)$ where $E$ is the stimulus energy and $E_0$ is the energy giving a half-maximal response. Gray lines are the asymptotes of the hyperbolic function. The stimulus energy for half saturation (corresponding to the intersection of the high- and low-energy asymptotes) is indicated by the arrow at 1.03 R*/rod, a typical value [mm207].

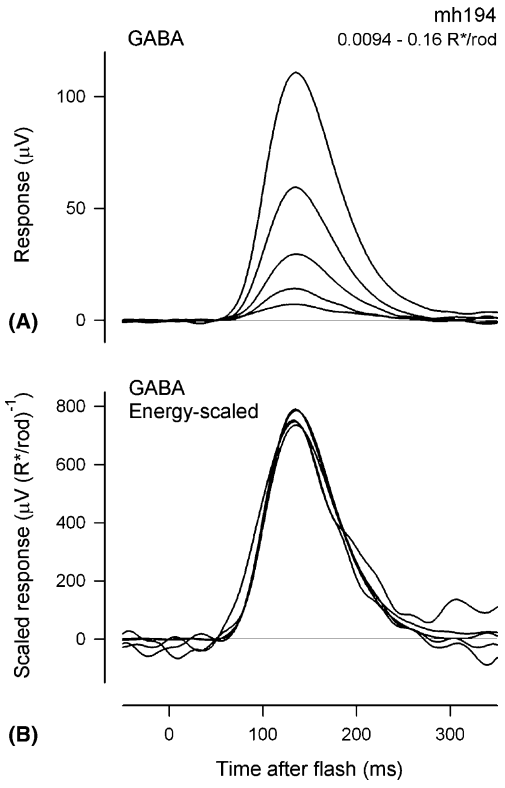


Fig. 5. Energy-scaled isolated PII. (A) ERG of a normal animal after intravitreal injection of GABA for five different stimulus energies increasing by factors of 2 starting with a stimulus giving an average of 0.0094 R*/rod. (B) The same responses after each response had been scaled by the energy of the stimulus that evoked it. The bandwidth of all the responses shown in this figure was digitally limited to 30 Hz [mh194 (GABA: 46 mM)].

terms) the response saturates in a way that is well described by the hyperbolic function of stimulus energy (continuous black curve with asymptotes shown in gray) that has commonly been used to fit b-wave data. As was the case in our previous studies of cat and mouse ERG, the ''corner'' of the saturation function (or equivalently, the half-saturating stimulus energy) was at approximately 1 R*/rod (Robson & Frishman, 1995; Saszik, Frishman, & Robson, 2002).

The impression that after GABA the complete waveform of responses to weak stimuli scales linearly with stimulus energy is best confirmed by plotting a set of records after scaling each of them by the stimulus energy at which the record was obtained. Fig. 5 shows such records both before (Fig. 5A) and after (Fig. 5B) energy scaling.

The energy-scaled records in Fig. 5B are all essentially identical, confirming that for these weak stimuli, increasing the stimulus energy produces a proportional increase in the amplitude of the response at all times after the stimulus. It should be noted that because the effect of energy scaling is to greatly increase the relative magnification of the responses to the weakest stimuli, these records are rather noisy despite having been digitally filtered to remove all components above 30 Hz.

### 3.5. Responses to stronger stimuli

It is important to examine whether the linear relationship between response amplitude and stimulus energy demonstrated above for bipolar cell (ERG) response to weak stimuli is altered when stimuli are strong enough to give rise to multiple photoisomerizations in some rods. Though the contributions from photoreceptors and cone bipolar cells are small enough to be neglected when examining ERG responses to weak stimuli, they become of greater importance when an increase in the stimulus energy makes it possible to examine the responses at earlier times (at which they are relatively larger). This can be appreciated by looking at Fig. 2D which shows ERG responses of a GABA-treated mouse to stimuli with energies producing up to 64 R*/rod.

Over most of the range of stimulus energies used to produce the set of records in Fig. 2D the leading edge of the positive wave rises directly from the baseline with the response to the weakest stimulus (0.038 R*/rod) only appearing after a latent period of around 70 ms. As the stimulus energy is increased the leading edge of the response moves steadily forward to earlier times, until finally (for the strongest two stimuli) a small a-wave becomes visible. The emergence of the a-wave for a stimulus energy giving 32 R*/rod can be seen more clearly in

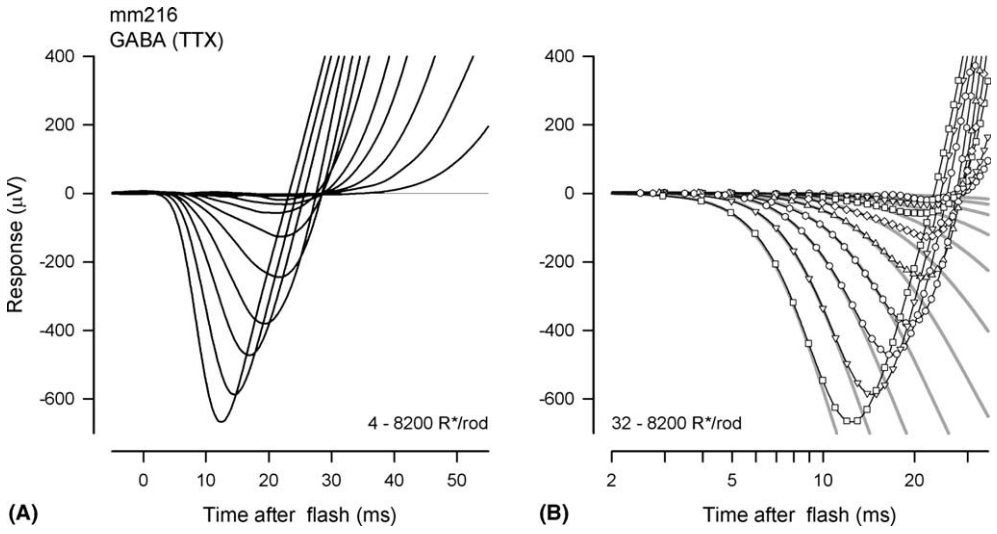


Fig. 6. The early part of isolated PII. (A) The early part of the ERG of a normal mouse after intravitreal injection of GABA (following an injection of TTX) for a range of stimulus energies increasing from 4 to 8200 R*/rod by factors of 2. The records were digitized at 1 kHz but the points are not shown in this part of Fig. 6. The continuous lines were obtained by Fourier interpolation as explained in Robson and Frishman (2004). Note that until the stimulus energy exceeds about 1000 R*/rod all records cross the zero line at about 28 ms. (B) The same recordings shown on a logarithmic time scale as open circles together with continuous lines generated by a model of photoreceptor response having the form described by Robson et al. (2003). The parameters of this model were: time constants of three stages of the transduction cascade, 45, 65 and 120 ms; time delay 3.9 ms provided by a gamma distribution function of order 12; exponential/hyperbolic nonlinearity factor, 0.7; $V_{max}$, −1200 μV [mm216].

Fig. 6A which shows the early part of responses to stimuli between 4 and 8200 R*/rod. Despite the apparent absence of an a-wave for some of these stimuli, it can be shown by averaging much larger numbers of responses, that even when the stimulus is much weaker, the b-wave is always preceded by an initial negative wave with a peak around 22 ms and a zero crossing about 28 ms after the stimulus (not illustrated here). The amplitude of this negative wave which is proportional to stimulus energy is just too small for the wave to be visible in normal recordings.

The time of the zero-crossing can be interpreted as the time at which the slowly rising negative response of the photoreceptors is exactly cancelled by the more delayed but faster rising positive response of the bipolar cells. This time will not change significantly with changes in stimulus energy if both signals are affected in the same way by increasing the energy, a condition achieved when both photoreceptors and bipolar cells respond linearly and the amplitude of their responses is proportional to the stimulus energy. Although the shape of the a-wave remains invariant for stimulus energies up to about 200 R*/rod, at higher stimulus energies the shape changes with the times of the peak and the zero crossing becoming progressively earlier (see Fig. 6A and B). In this range of times and stimulus energies, as well as for lower stimulus energies at later times when the amplitude is sufficiently great, changes in waveform will result from nonlinear (saturating) operation.

Since it can be assumed that the earliest part of the leading edge of the a-wave is provided by the photoreceptors alone, it is possible to analyze the recordings to estimate the parameters of a model of the photoreceptor component of the ERG (as described by Robson et al., 2003). This model can then be used to compute the amplitude of the photoreceptor component at later times when it is summed with responses from other cells. The gray lines in Fig. 6B show the fit of such a model obtained by adjusting the parameters to the values given in the figure legend. Although the model was developed to describe the rod photoreceptor contribution to the macaque ERG, the same formulation with only slightly different parameters provides a good a fit to the initial 80% of the rising edge of the mouse mixed (rod and cone) dark-adapted a-wave for times up to about 15 ms. We have also found (not illustrated) that the same model provides an acceptable description of about the first 80 ms of the ERG recorded from *nob* mice that have no depolarizing bipolar cell response (Pardue, McCall, LaVail, Gregg, & Peachey, 1998).

We can now examine the bipolar cell responses to stimuli whose energy is great enough to produce a significant photoreceptor contribution. This is done by subtracting our modeled estimates of the photoreceptor response from the whole ERG. These records will be referred to as "isolated PII", as they were in previous studies of the cat ERG (Robson & Frishman, 1995).

Fig. 7A shows the same recordings as shown in Fig. 2D from a GABA-treated mouse eye, but also includes (as dashed gray lines) the corresponding photoreceptor components estimated as described in the text above. It is clear that the a-waves that are visible with the

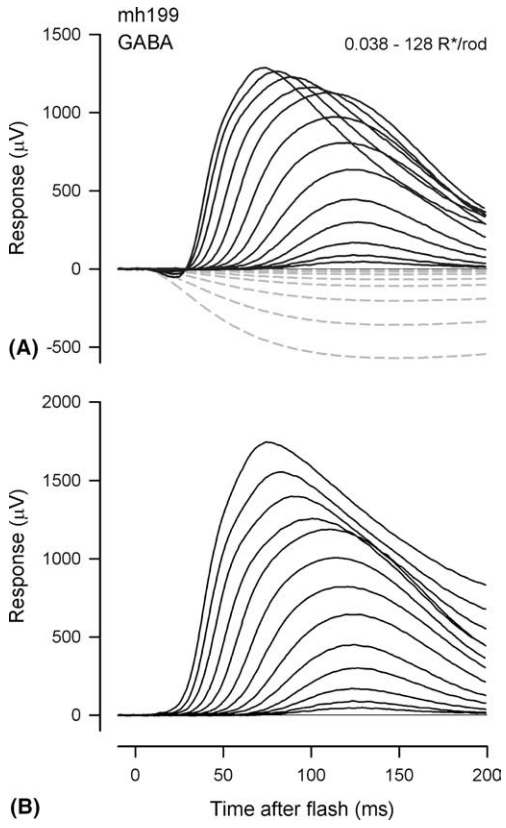


Fig. 7. Estimating the photoreceptor component. (A) The ERG of a normal mouse after intravitreal injection of GABA for stimuli with energies increasing from 0.038 to 128 R*/rod by factors of 2. Note that although an overt awave is only visible for the two strongest stimuli, the photoreceptor component for the strongest stimulus has a peak amplitude of about 650 μV. (B) Isolated PII. The same ERG recordings as in (A) after subtracting the photoreceptor component estimated from fitting a model to the leading edge of the awave as shown (for a different animal) in Fig. 6B [mh199].

strongest stimuli represent only a small part of the photoreceptor component, and that photoreceptors contribute substantially to the later part of the ERG even when no a-wave is visible. After the photoreceptor component has been subtracted from the ERG to reveal isolated PII (Fig. 7B), it can be seen that the saturation of PII is less abrupt than in the original ERG, and that the front edge of the bipolar cell response occurs progressively earlier with increasing stimulus energy over this whole range. It is not, however, possible to tell from this plot whether there is a true reduction in latency with increasing stimulus energy. The shortening of the time required for the response to become visible, or to reach any given criterion level, could also be a reflection of the increase in amplitude of the response at early times.

### *3.6. Energy-scaled responses and the energy-scaled response envelope*

Because ERG recordings are inevitably contaminated by noise, it is not possible to determine the timecourse of the early part of responses to stimuli that are small enough for the bipolar cells to be operating completely linearly because the early part is lost in the noise. However, as recognized by Baylor, Hodgkin, and Lamb (1974) in studies of single turtle cone responses, the timecourse of the early part of the response of any system which operates linearly up to the level at which it saturates can be determined by recording responses both to weak stimuli for which the operation is completely linear and to strong stimuli which send the system into saturation. If each of the recorded responses is scaled by the stimulus energy at which it was obtained then, up to the time at which the response amplitude grows large enough for the effects of saturation to become significant, the energy-scaled responses will be identical. This means that there will be, for each stimulus energy, some different portion of the response that is large enough for the noise to be of little consequence but is still small enough to avoid saturation and be approximately linear. The timecourse of the unsaturated energy-scaled response over the full time range can then be obtained by combining the various portions for which operation was linear. In practice the range of each of the appropriate portions is not known precisely. However, superimposing sets of energy-scaled records will reveal which portions of the different responses should be combined, as these will form the envelope of the response set (e.g. Robson et al., 2003).

Although this approach is most obviously applicable when the system operates completely linearly at early times after a stimulus, as described above, the same approach can still be applied when there are nonlinearities involved, and indeed may be useful in revealing such nonlinearities. Fig. 8A and B show the isolated PII data of Fig. 7B after energy-scaling. They are plotted on linear and double logarithmic axes respectively.

The top three curves in these plots, generated in response to the weakest stimuli, (0.038, 0.075 and 0.15 R*/rod, indicated by open circles) are, like the curves in Fig. 5, all essentially superimposed, confirming that, for this range of stimulus energies, the retina is operating linearly in the sense that the response amplitude is proportional to stimulus strength. On the other hand, when the stimulus energy is increased beyond this level the energy-scaled response starts to saturate and the peak amplitude of the energy-scaled response becomes reduced. At a stimulus level not much higher than this, certainly by the time the stimulus produces an average of 0.5 R*/rod (at which stage there will be 2 or even more photoisomerizations produced in some rods), the initial portion of the leading edges of the individual responses have also started to change shape, moving steadily earlier as the stimulus energy is raised. This effect can be seen in Fig. 8A in the range indicated by the arrow but is most easily seen in the double logarithmic plot (Fig. 8B) which provides an effectively magnified view of the lower and earlier part of the curves.

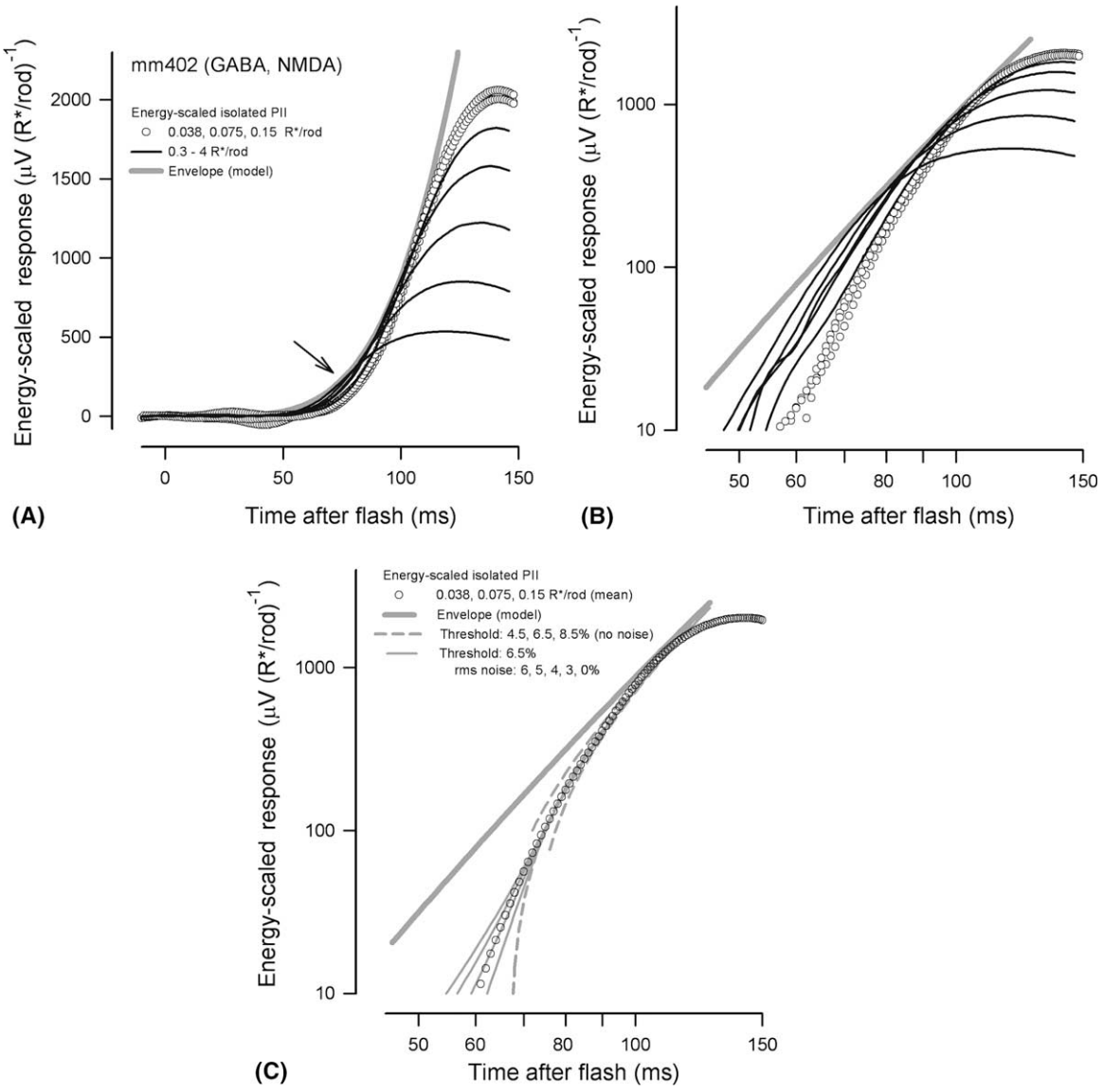


Fig. 8. Energy-scaled isolated PII. (A) Energy-scaled isolated PII for various stimulus energies. Open circles plot responses to weak stimuli with energies of 0.038, 0.075 and 0.15 R*/rod, black lines plot responses to stronger stimuli with energies of 0.3, 0.5, 1, 2 and 4 R*/rod. The nearly straight gray line forming the envelope of the leading edge was generated by the six-stage model of bipolar cell response described in the text. The arrow indicates the region where the responses to weak stimuli fall below the envelope. (B) The same data plotted on double logarithmic axes. (C) The open circles plot the mean of the energy-scaled responses obtained with stimuli having energies of 0.038, 0.075 and 0.15 R*/rod. The thick gray line is the model fit to the envelope of responses to stronger stimuli. Narrow dashed gray lines show model responses for thresholds of 4.5%, 6.5% and 8.5% of the peak amplitude (2000 μV (R*/rod)$^{-1}$) without noise. Continuous narrow gray lines show predictions of a model having a threshold at a level of 6.5% of the peak amplitude with added noise having an rms amplitude 6%, 5%, 4% and 3% of the peak value. [mm402]

Although each of the individual energy-scaled response curves has a short portion between a steeper initial segment and a later shallower one that falls on a common locus corresponding to the gray line, the initial portions of all responses other than those generated by the weakest stimuli, are obviously not superimposed. This indicates that the initial portion of each of these responses involves some nonlinear operation of threshold type. Moreover, the fact that this effect is only observed at stimulus levels that give rise to multiple photoisomerizations in individual rods is consistent with the nonlinearity existing in the connections between individual rods and bipolar cells rather than after summation by the bipolar cells of signals from several rods.

### 3.7. "Fifth power" law

Although the responses to weak stimuli start to rise later than the responses to stronger stimuli and then rise relatively more steeply, the leading edges of the whole set of curves generated by stimuli whose energies cover a wide range (about 100:1 in this figure) are bounded

by an envelope which in the plot with double logarithmic coordinates (Fig. 8B) is almost straight. A similar observation was made by Robson and Frishman (1995) in their study of isolated PII in the cat. They described the envelope of the energy-scaled responses with a simple power-law of the form $V = k(t - t_d)^5$, where the voltage, $V$, rises, after a delay of $t_d$, as the fifth power of the elapsed time. The value of the exponent, 5, was interpreted to indicate that the recorded response was generated by a system involving six successive stages of temporal integration, three in each of the phototransduction and synaptic cascades. It has subsequently become clear that the response of the phototransduction cascade is better described by a three-stage low-pass filter with finite time constants (Robson et al., 2003). We have therefore chosen to describe the envelope of the energy-scaled isolated PII records by a relation that assumes that the response of the rods is that of a three-stage low-pass filter having time constants of 45, 70 and 120 ms and that this is followed by three stages of integration resulting from the operation of the synaptic cascade. In this case the time delay, $t_d$, has been set to a value of 4.1 ms (this being the sum of the delay in the recording amplifier and that in the phototransduction process as determined by fitting a model for the rod response to the early part of the ERG). The only free parameter of this model, the scaling constant $k$, has been adjusted to make the line fit the envelope of the uppermost curves.

### 3.8. Threshold level

In an ideal system which is linear aside from an ideal threshold element (zero transmission below the threshold and unity transmission above it) at its output and is transmitting continuous noise-free signals, we would expect to see no output at all following a brief stimulus until the internal signal presented to the threshold element had built up to the level to which the threshold is set. At this time (i.e. after some absolute latent period) the measured output would suddenly start to rise, thereafter having an amplitude equal to the difference between that of the signal reaching the threshold mechanism and the level to which the threshold was set. A log–log plot of this measured output would, at some definite time after the stimulus, start to rise almost vertically and would then asymptotically approach the curve that would have been obtained if there had been no threshold (i.e. if the threshold level had been zero). In this case the threshold level could be exactly estimated as the amplitude of the internal response at the time that an overt response could first be recorded. Fig. 8C shows (three dashed gray lines) the energy-scaled response that would be expected if the threshold level were 4.5%, 6.5% or 8.5% of the peak amplitude and the response with no threshold is given by the envelope (model) curve. It can be seen that the average energy-scaled response to weak stimuli (open circles) corresponds closely over its upper portion to what would be expected with a threshold level of about 6.5%. However, at earlier times, the measured amplitude followed a path that did not correspond to any particular threshold level.

This discrepancy can be explained if we take into account that the signal reaching the threshold element is not free of noise but includes noise components originally present in the signals from the rods as well as components generated by the quantal nature of the synaptic process and the operation of the synaptic cascade. Assuming that the noise has a Gaussian amplitude distribution we can calculate the average output that would be expected for various amplitudes of the added noise. The thinner gray lines in Fig. 8B show the effects on the recorded response of adding noise whose rms amplitude is 6%, 5%, 4% or 3% of the peak amplitude of the single-photon response. In this case the amplitude of the recorded response at early times corresponds to that expected if the added noise had an rms amplitude of about 4% of the peak response, i.e. about 60% of threshold level of 6.5% of the peak.

Recordings obtained from four other animals all indicated a threshold of less than 10% of the amplitude of the single-photon response and an rms noise amplitude of some lower value.

### 3.9. Rod and cone bipolar cells

Although the envelope of the energy-scaled responses with stimulus energies up to 4 R*/rod that are shown in Fig. 8 could be adequately described by a ''fifth power'' model, responses to stronger stimuli did not fit so well. This can be seen in Fig. 9A which shows the same energy-scaled responses as Fig. 8 but also includes responses to stronger stimuli (8, 16 and 32 R*/rod, plotted as open circles). As was typical for all the normal animals we studied, the responses to the stronger stimuli rose somewhat earlier than the model curve. It can also be seen that the leading edges of the responses to stronger stimuli (e.g. the lowest three curves in Fig. 9A) run parallel to the model line and do not steepen at early times, as occurred for responses to the weaker stimuli. While the difference in timecourse between the responses to the weaker and the stronger stimuli might indicate some general inappropriateness of the model as a description of rod bipolar cell responses in the mouse, it seems more likely that it reflects the presence for the stronger stimuli of a contribution from another cell type: i.e. the cone bipolar cells. It is an implication of this hypothesis that the response of the cone bipolar cells would rise and peak considerably earlier than that of the rod bipolar cells so that the cone bipolar cell contribution would have little effect in shaping the overall response at later times.

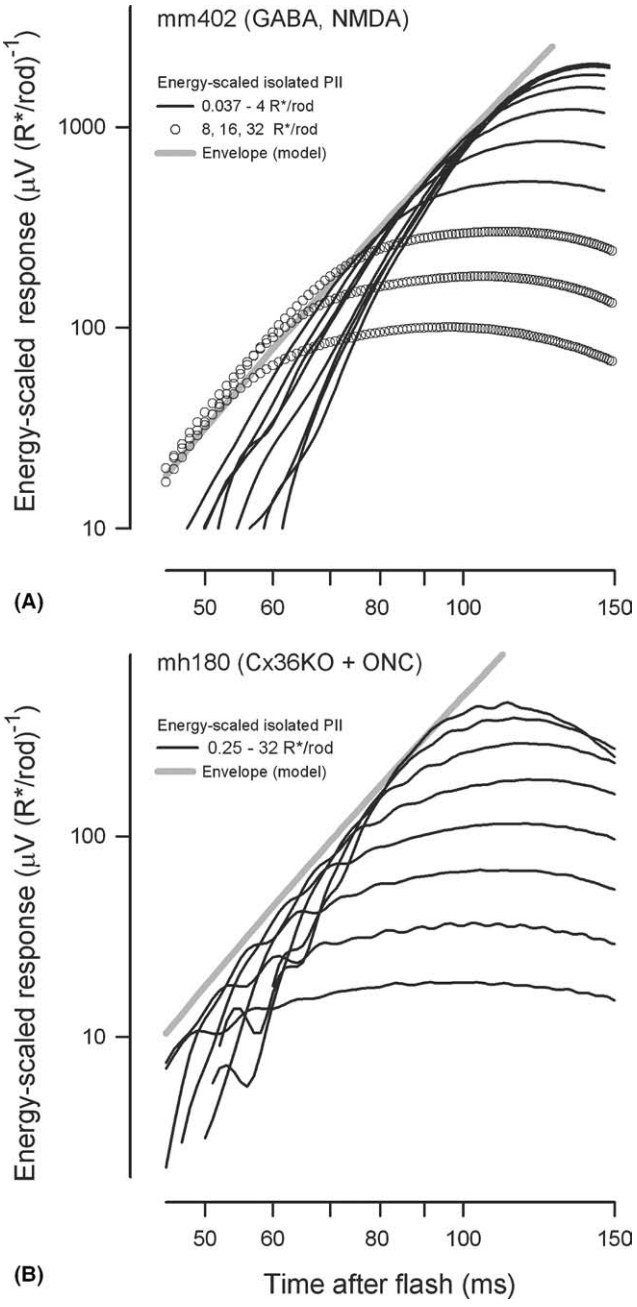


Fig. 9. Energy-scaled isolated PII from a normal and a Cx36 KO mouse. (A) Energy-scaled isolated PII from a normal mouse for various stimulus energies. Black lines plot responses to stimuli with energies between 0.038 and 4 R*/rod (same records as shown in Fig. 8), open circles show responses to 8, 16 and 32 R*/rod. The thick gray line is a model curve generated by the six-stage model of bipolar cell response described in the text [mm402]. (B) Energy-scaled ERG responses from a Cx36 KO mouse having a crushed optic nerve for a range of stimulus energies increasing from 0.25 to 32 R*/rod by factors of 2. The thick gray line is a model curve generated by the six-stage model of bipolar cell response described in the text [mh180].

To examine the hypothesis that cone bipolar cells, and specifically the rod- (rather than cone-) driven signal in cone bipolar cells might be contributing to the ERG evoked by the stronger stimuli, we recorded responses from Cx36 KO mice which lack functional gap junction connections between rods and cones. Fig. 9B shows a set of energy-scaled ERG responses from such a knockout mouse.

Although there was a small residual oscillatory component present in every record, the envelope of the leading edges of the records conformed quite closely with the same power-law curve that was fitted in Fig. 8A and B to the responses to weaker stimuli of normal mice. Over the whole range of stimulus energies (0.25–32 R*/rod), the general form of the leading edge of the each responses was (ignoring the oscillatory component) quite similar. At each energy, the response coincided with the envelope only over a short range and was steeper at shorter times. Although in the normal animal (Fig. 7B) the same thing is true of responses to weaker stimuli, the initial part of the individual responses to stronger stimuli rises as predicted by the "fifth power" relation. The results for another Cx36 KO animal was very similar.

Taken together, the observed differences between ERG responses of normal and Cx36 KO mice suggest that the ERG of the latter animals is missing a rod-driven contribution from cone bipolar cells whose activation does not involve a threshold nonlinearity.

### 3.10. "Supralinearity" of rod bipolar cell response

When measurements are made at any relatively long time after the stimulus at which all energy-scaled responses fall on or below a value defined by responses to the weakest stimulus (e.g. at the peak of the response), the amplitude must initially increase in proportion to stimulus energy before eventually saturating. Fig. 4 shows how response amplitude measured at the time of the peak of PII (about 110 ms after the stimulus flash) increases in this way with stimulus energy. At earlier times, when energy-scaled responses to the weakest stimuli fall below the envelope (see Fig. 8A and B), there must be some region in the amplitude versus energy relation where the amplitude rises more steeply than in proportion to stimulus energy.

This kind of "supralinearity" is clearly seen in Fig. 10A and B which show, as a function of stimulus energy, the amplitude of the b-wave (measured from the baseline without correction for the photoreceptor component of the ERG) in two GABA-treated animals at various different times after the stimulus. The dashed gray lines that have been plotted to be tangential to the measured amplitude just prior to the onset of saturation indicate what would have been expected if the response had increased completely linearly up to this level. At a time just prior to that of the peak of the response (110 ms in Figs. 4 and 10A and 115 ms in Fig. 10B) the response amplitude did indeed rise linearly with stimulus energy (i.e. with a slope of 1 on this

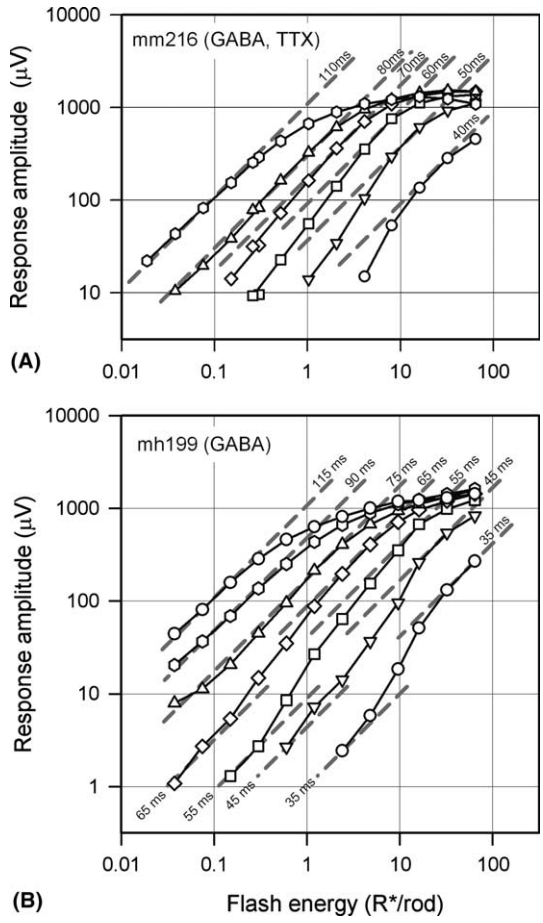


Fig. 10. The amplitude of the positive wave of the ERG of two normal mice after intravitreal injection of GABA (photoreceptor component not subtracted) measured at various times after the stimulus and plotted as a function of stimulus energy. Gray lines show linear relationship. (A) The intravitreal injection of GABA was given following an earlier injection of TTX. 20 responses were averaged [mm216]. (B) Amplitudes were measured from averages of 40 responses. Lower gray lines show linear relationship that was approached when the responses amplitude was less than about 3 μV [mh199].

double-logarithmic plot) up to the level at which saturation set in. However, when the amplitude was measured at 70 ms, or earlier, it rose significantly more steeply than this over a substantial portion of its range. At earlier times the steeply rising portion of the curve occurred over a higher range of stimulus energies.

Although the amplitude versus energy functions measured at early times all showed an obvious section over which the amplitude increased more rapidly than in direct proportion with stimulus energy, when the response amplitudes was less than about 3 μV, the amplitude was proportional to stimulus energy even at early times (lower gray lines in Fig. 10B).

The measurements made at 80 and 75 ms (Fig. 10A and B) are of interest because, although the slope of these curves did not certainly exceed unity over any range, it appeared that the very nearly linear behavior extended to greater amplitudes than at times nearer that of the peak. This extended linear region may have arisen as a result of the mutual cancellation of a slope reduction due to saturation with a "supralinearity" effect due to the threshold.

### 3.11. Time of response

The time for a retinal response to reach any chosen criterion level will depend upon the stimulus energy while the nature of this dependence will be determined by the timecourse of the response and the way this is altered by stimulus energy. If the response rises as a power-law function of time, and the response amplitude is proportional to stimulus energy (as is a reasonable approximation in the case of photoreceptor and bipolar cell signals over much of their range) there will be a very simple relation between the time to reach a given criterion level and stimulus energy. After allowing for any fixed delay, we can expect that the time for the response to reach a criterion level will be inversely proportional to the power of the stimulus energy where the exponent will be the reciprocal of that relating amplitude to time after the stimulus. Thus, in the case of the response of rod bipolar cells which rises after a short delay approximately as $t^5$, the time to reach a criterion level can be expected to decrease as $E^{1/5}$, where $E$ is the energy of the stimulus (see Robson & Frishman, 1995).

The introduction of a threshold nonlinearity between the mechanism that establishes the kinetics of the cells' internal response and its manifestation in the ERG (e.g. between the concentration of an internal messenger and the bipolar cell's membrane conductance) will not affect this relationship though it will affect the actual time required for the ERG to reach any particular criterion level.

Fig. 11A shows the lower part of the leading edges of a set of isolated PII responses from a normal mouse (after intravitreal injection of TTX and then GABA). The voltage is plotted as a function of the logarithm of the time after the stimulus to emphasize the quite regular relative decrease in the time that is produced by each doubling of the stimulus energy.

The relation between time-to-criterion and stimulus energy is plotted in Fig. 11B for the three criterion levels shown in Fig. 11A (40, 160 and 640 μV). A fixed transport delay estimated as 4.5 ms from fitting the leading edge of the a-waves with a model as shown in Fig. 6B, has been subtracted from all times. The dashed gray lines all have a slope on this log–log plot of −1/5. Despite some irregularity in the data it appears that the time-to-criterion is well described at all three criterion levels and over very nearly the whole range of stimulus energies by a power law with an exponent of −1/5. Plots of this nature for four other animals treated with GABA as well as in two Cx36 KO animals were similar.

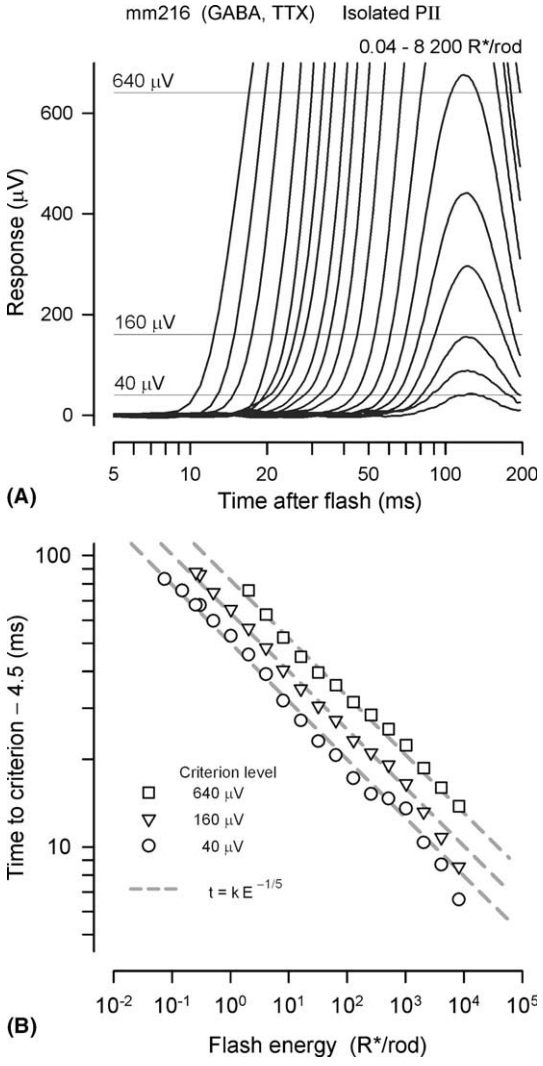


Fig. 11. Time required for isolated PII to reach criterion response levels. (A) Early part of isolated PII of a normal mouse for a wide range of stimulus energies (0.04–8200 R*/rod) showing criterion response levels of 40, 160 and 640 μV. (B) Time required for isolated PII of a normal mouse to reach criterion levels of 40, 160 and 640 μV as a function of stimulus energy. The dashed gray lines all have log–log slopes of −1/5, i.e. they plot $t = kE^{-1/5}$ [mm216].

## 4. Discussion

In this paper, we have studied the transmission of photon signals from rods to rod bipolar cells by recording the rod bipolar cell component of the mouse ERG. The ganzfeld ERG provides a unique opportunity to study, in a nearly physiological preparation, responses of the retina operating near the absolute limit of sensitivity. This is because the gross response that constitutes the ERG is the sum of the responses of individual cells over the entire retina, allowing us to see a response when less than 1 in 10,000 rods has absorbed a single photon. We believe that the ERG response that we are attributing to rod bipolar cells is correctly ascribed because we have isolated it both with pharmacological agents and by eliminating more sensitive inner-retinal components with genetic manipulation and optic nerve section. We demonstrated, in Fig. 3, the similarity in timecourse between the isolated PII response in the ERG and single-cell current recordings in a slice preparation. Further, we found that the leading edge of the response can be described by a kinetic function that takes into account only the transduction cascade of the photoreceptors and that of the synapse from photoreceptors to depolarizing bipolar cells.

### 4.1. Existence of a threshold nonlinearity

Field and Rieke (2002), working in the mouse retinal slice preparation, based their conclusion that there is a threshold mechanism operating prior to the generation of post-synaptic current by rod bipolar cells upon their observation of a "supralinearity" in the rise of the average peak amplitude of bipolar cell responses with increasing number of stimulus photons. We did not observe such behavior of the peak amplitude of the rod bipolar cell component (isolated PII) of the ERG, although supralinearity did occur at times much earlier than the peak (see below). (Berntson, Smith, & Taylor, 2004, working in a retinal slice preparation in mouse also did not observe the supralinearity at the peak of the response). Our ERG measurements indicate that when no more than a small proportion of the rods in a rod bipolar cell's receptive field are activated by single photons, the average peak amplitude of the bipolar cell's response initially rises in exact proportion to the number of photons in the stimulus and the whole response waveform simply scales with stimulus energy (Figs. 4 and 5). When more than a few rods are activated, rather than rising faster than it did initially, the peak amplitude rises more slowly as saturation sets in (Fig. 4). It should be emphasized that the linear relationship between ERG amplitude and stimulus energy that is found for these weak stimuli does not imply that the retinal elements contributing to the response are operating linearly, but only, as pointed out by Cone (1963), that the amplitude of the summed responses of all rod bipolar cells necessarily must be proportional to the number of rod bipolar cells that are activated.

Although the peak amplitude of isolated PII starts off by increasing in exact proportion to stimulus energy, this is not what we observed when the amplitude was measured at times substantially earlier than the peak (Fig. 10). At times early enough for the amplitude at low energies to be little more than about one tenth of the value at the time of the peak (i.e. earlier than 70–75 ms after the stimulus), there was a range of stimulus energies over which the amplitude increased more rapidly than in direct proportion to increasing stimulus energy (i.e. "supralinearly") before ultimately showing

saturation. The existence of this supralinear range indicates the existence of a threshold nonlinearity in the transmission of single-photon signals from the rods to the rod bipolar cells, and that the level of the threshold is less than about one tenth of the peak amplitude of the single-photon response.

### 4.2. Estimation of threshold level

We have estimated more precisely the level to which this threshold is set by examining the timecourse of the rising edge of isolated PII when the stimulus was weak enough for the response to be generated by single photoisomerizations in only a small proportion of rods. Based on the assumptions that (a) the timecourse of the signal presented to the threshold element is that of the envelope of the rising edges of the energy-scaled responses as described by the six-stage model (Fig. 8B and C), (b) that the threshold is an abrupt one, with zero transmission below, and unity transmission above, the set level, and (c) that the amplitude of any additive noise in the system is relatively low, we could predict the timecourse of the recorded single-photon response by subtracting a value equal to the threshold from the pre-threshold signal and ignoring negative values. In each animal it was possible to obtain a satisfactory description of the empirically determined timecourse of (isolated) PII over a substantial range of higher response amplitudes with a model of this kind having a threshold set to a level of 10%, or less, of the peak amplitude of the single-photon response. However, as addressed just below, in no case did we see the steep rise in the response that this model predicts at early times (e.g. Fig. 8C).

### 4.3. Effect and amplitude of the noise

Absence of a steep rise of PII amplitude at times when the internal pre-threshold signal has just exceeded the threshold level could occur either because the signal that reaches the threshold mechanism is noisy (and will therefore sometimes exceed the threshold before the noise-free signal has reached the threshold level), or because the transmission characteristic of the threshold mechanism changes from zero to unity over an appreciable range of the input rather than at some particular input level. The effects of these two possibilities are indistinguishable and both may well be operative; however, we chose to assume that the effect is produced entirely as a result of added noise so that we could obtain a maximum estimate of the noise amplitude. We calculated the average amplitude of the signal plus noise that exceeds the threshold value for different values of the noise and compared these predictions with the measured amplitude at early times (Fig. 8C). In each of the three animals for which we obtained adequate measurements the rms amplitude of the noise that was necessary to explain the observed timecourse of isolated PII at early times was about 2/3 (0.5–0.8) of the threshold level.

### 4.4. The underlying mechanism and location of the threshold nonlinearity

Examination of the effects of pharmacological agents upon the responses of rod bipolar cells in mouse retinal slices (Sampath & Rieke, 2004) has indicated that the threshold is the result of a saturation effect at some stage in the post-synaptic transduction cascade in the rod bipolar cells. Although our ERG studies can provide no information about the mechanism of the threshold, they can provide information about the location of the threshold. This possibility arises because each successive stage of the synaptic machinery introduces some change in the kinetics of the signal. For this reason the operation of a threshold nonlinearity at any one of the stages that are involved will have a characteristic effect on the overall kinetics of the bipolar cell response, either as measured directly or as a component of the ERG. Our observations indicate, in agreement with the conclusions of Sampath and Rieke (2004), that the threshold nonlinearity is associated with the operation of the synaptic cascade and must, in fact, be located downstream of all those stages of the cascade that affect the timecourse of the response. We base this conclusion on our finding that the time required for the response to reach some criterion level decreased with increasing stimulus energy in the same way when measured with a low criterion level as with higher levels.

The time delay of the PII response decreased, after the small fixed time introduced by the rods, as the stimulus energy raised to the power of 1/5. As explained by Robson and Frishman (1995) this is the expected relationship when the rod bipolar cell response rises as the fifth power of the time after the stimulus and the response amplitude is proportional to stimulus energy. Although this very simple power law is not exactly correct (see Section 3), the simple fifth power law is a good approximation except at the very longest times, and provides the basis for an acceptable fit to our latency measurements (Fig. 11B). Although the situation is a little less simple if there is a threshold nonlinearity operating at the output of the pathway, the presence of such a nonlinearity does not affect the relationship between latency and stimulus energy for any given criterion level. However, if the threshold is located between the output of the transduction cascade in the rod and the input of the synaptic cascade in the bipolar cell, the time to reach a low criterion level (i.e. comparable to the threshold level itself) will primarily be determined by the kinetics of the rods alone. Since the rod signal rises approximately as the square of the time after the stimulus (Lamb & Pugh, 1992; Robson et al., 2003), the time for the bipolar cell output to reach a low criterion level

would decrease as the square root of stimulus energy. In contrast, the time to reach a criterion level much greater than the threshold would continue to be determined largely by the overall kinetics and would therefore be inversely related to the one fifth power of stimulus energy. A threshold operation occurring at an intermediate stage in the synaptic cascade would produce a relationship intermediate between a square root and a one fifth power law. We did not observe a difference in the relationship between delay time and stimulus energy at different criterion levels, and therefore predict that the threshold operation occurs after all stages that affect the kinetics of the bipolar cell response.

### 4.5. Functional significance of a threshold nonlinearity

Our findings differ substantially from those of Field and Rieke (2002) not only with respect to the level of the threshold at the rod to rod bipolar cell synapses, but also with respect to the (predicted) amplitude of the noise which contaminates single-photon signals reaching these synapses. In both cases, our values for the intact retina were lower than those found in the retinal slice.

Even if the continuous noise that contaminates single-photon signals from the rods were much lower than was measured by Field and Rieke (2002), there would be still be a functional requirement for a threshold at the rod to rod-bipolar cell synapse. However low the amplitude of the noise at the output of each rod relative to single-photon responses is, after simple linear addition by a bipolar cell of the outputs of many rods the noise level relative to a single-photon signal would be substantially higher (five times higher if signals from 25 rods were added). The introduction of a threshold at the rod to rod bipolar cell synapse, even a threshold with a level as low as we have found, could serve to restore the signal-to-noise ratio of the summed rod signals. In this context it is interesting to note that if a Gaussian noise of unit amplitude is passed through a simple threshold element that only transmits when the signal amplitude is greater than 1.65, which is approximately the ratio of threshold level to rms noise amplitude that we observed, then the rms amplitude of the transmitted noise is 1/5. This suggests that the threshold at the rod to rod bipolar cell synapse serves to maintain the signal-to-noise ratio at the output of the bipolar cells at essentially the same value as that of the inputs from the rods.

The location of the thresholding operation at the output of the cascade in the rod bipolar cell is appropriate if the threshold serves to maintain the signal-to-noise ratio at this stage in the rod pathway in the face of noise that is generated not only by operation of the transduction cascade in each rod, but also as a result of the quantal nature of transmitter release from the rods and of the operation of the synaptic cascade within the bipolar cell dendrites (van Rossum & Smith, 1998).

### 4.6. Rod signals traveling via rod vs. cone bipolar cells

While the direct synaptic connections between the rods and rod bipolar cells provide the pathway that is involved in transmitting single-photon signals from the rods and is essential to maintaining high sensitivity at very low light levels, signals from rods are also transmitted via gap junctions to adjacent cones and hence to other (cone) bipolar cells. This secondary pathway provides a route for signals evoked by stimuli that are strong enough to activate more than a few of the rods in the receptive field of each rod bipolar cell; such stimuli are not well represented by the responses of rod bipolar cells because these will be at least partially saturated. This pathway creates problems when studying the ERG component from rod-activated rod bipolar cells at higher light levels because of the contribution of the response simultaneously generated by rod-activated cone bipolar cells. Because there is no practicable way to differentially block the responses of depolarizing rod and cone bipolar cells pharmacologically, we have assessed the magnitude of the ERG contribution of the secondary pathway by comparing the responses of normal animals with those of lacking connexin36, and therefore without functional gap junction connections between rods and cones (Guldenagel et al., 2001; Deans et al., 2002).

In normal animals (for the stronger stimuli) the leading edge of energy-scaled responses on log–log coordinates occurred at slightly earlier times that that predicted by our kinetic model for the leading edge of the rod-driven bipolar cell response in the ERG, but followed the six-stage filter model over a substantial range of times. Over the range of stimulus energies that we studied, there was no sign of supralinearity in these "early" responses. In contrast, in the Cx36 KO animals, this extra earlier portion of the response was absent. On the assumption that the extra component in the ERG of normal animals is generated by rod-driven cone bipolar cells, the adherence of the "early responses" to the six stage model suggests that there is no threshold in the pathway from rods (via gap junctions) to cones and thence in synaptic activation by photoreceptors of cone bipolar cells. Of course this prediction needs to be tested by recording from single cone bipolar cells.

## Acknowledgments

We thank Dr. Micheal Deans and Dr. David Paul for the Cx36 KO mice.

Support: NIH Grants RO1 EY06671, P30 EY07551, T32 EY07024.

## References


Baylor, D. A., Hodgkin, A. L., & Lamb, T. D. (1974). The electrical response of turtle cones to flashes and steps of light. *Journal of Physiology, 242*, 685–727.

Baylor, D. A., Nunn, B. J., & Schnapf, J. L. (1984). The photocurrent, noise and spectral sensitivity of rods of the monkey *Macaca fascicularis*. *Journal of Physiology, 357*, 575–607.

Berntson, A., Smith, R. G., & Taylor, W. R. (2004). Transmission of single photon signals through a binary synapse in the mammalian retina. *Visual Neuroscience*, 21, in press.

Cone, R. A. (1963). Quantum relations of the rat electroretinogram. *Journal of General Physiology, 46*, 1267–1286.

Dawson, W. W., Trick, G. L., & Litzkow, C. A. (1979). Improved electrode for electroretinography. *Investigative Ophthalmology and Visual Science, 18*, 988–991.

Deans, M. R., Volgyi, B., Goodenough, D. A., Bloomfield, S. A., & Paul, D. L. (2002). Connexin36 is essential for transmission of rod-mediated visual signals in the mammalian retina. *Neuron, 36*, 703–712.

Field, G., & Rieke, F. (2002). Nonlinear signal transfer from mouse rods to bipolar cells and implications for visual sensitivity. *Neuron, 34*, 773–785.

Guldenagel, M., Ammermuller, J., Feigenspan, A., Teubner, B., Degen, J., Sohl, G., et al. (2001). Visual transmission deficits in mice with targeted disruption of the gap junction gene connexin36. *Journal of Neuroscience, 21*, 6036–6044.

Lamb, T. D., & Pugh, E. N. (1992). A quantitative account of the activation steps involved in phototransduction in amphibian photoreceptors. *Journal of Physiology, 449*, 719–758.

Li, Y., Schlamp, C. L., & Nickells, R. W. (1999). Experimental induction of retinal ganglion cell death in adult mice. *Investigative Ophthalmology and Visual Science, 40*, 1004–1008.

Pardue, M. T., McCall, M. A., LaVail, M. M., Gregg, R. G., & Peachey, N. S. (1998). A naturally occurring mouse model of X-linked congenital stationary night blindness. *Investigative Ophthalmology and Visual Science, 29*, 2443–2449.

Robson, J. G., & Frishman, L. J. (1995). Response linearity and kinetics of the cat retina: the bipolar cell component of the dark-adapted electroretinogram. *Visual Neuroscience, 12*, 837–850.

Robson, J. G., & Frishman, L. J. (1998). Dissecting the dark-adapted electroretinogram. *Documenta Ophthalmologica, 95*, 187–215.

Robson, J. G., & Frishman, L. J. (2004). Sampling and interpolation of the a-wave of the electroretinogram. *Documenta Ophthalmologica, 108*, 171–179.

Robson, J. G., Saszik, S. M., Ahmed, J., & Frishman, L. J. (2003). Rod and cone contributions to the *a*-wave of the electroretinogram of the dark-adapted macaque. *Journal of Physiology, 547*, 509–530.

Sampath, A. P., & Rieke, R. (2004). Selective transmission of single photon responses by saturation at the rod-to-rod bipolar synapse. *Neuron, 41*, 431–443.

Saszik, S. M., Frishman, L. J., & Paul, D. (2002). Effect on the rod-driven electroretinogram of eliminating connexin36 from the mouse retina. Society for Neuroscience Abstract. Number 236.8.

Saszik, S., Frishman, L. J., & Robson, J. G. (2002). The scotopic threshold response of the dark-adapted electroretinogram of the mouse. *Journal of Physiology, 543*, 899–916.

Sterling, P., Freed, M. A., & Smith, R. G. (1988). Architecture of the rod and cones circuts to the On-beta ganglion cell. *Journal of Neuroscience, 8*, 623–642.

Tsukamoto, Y., Morigiwa, K., Ueda, M., & Sterling, P. (2001). Microcircuits for night vision in mouse retina. *Journal of Neuroscience, 21*, 8616–8623.

van Rossum, M. C., & Smith, R. G. (1998). Noise removal at the rod synapse of mammalian retina. *Visual Neuroscience, 15*, 809–821.

Viswanathan, S., Frishman, L. J., Robson, J. G., Harwerth, R. S., & Smith, E. L. III, (1999). The photopic negative response of the macaque electroretinogram: reduction by experimental glaucoma. *Investigative Ophthalmology and Visual Science, 40*, 1124–1136.

Wässle, H., Grünert, U., Chun, H.-H., & Boycott, B. B. (1995). The rod pathway of the macaque monkey: identification of AII-amacrine cells with antibodies against calretinin and cortical magnification factor in the primate. *Vision Research, 30*, 1897–1911.